International Journal of Biological Macromolecules 134 (2019) 695–703

Contents lists available at ScienceDirect

International Journal of Biological Macromolecules

journal homepage: http://www.elsevier.com/locate/ijbiomac

Development of a reliable microRNA based electrochemical genosensor for monitoring of miR-146a, as key regulatory agent of neurodegenerative disease

Balal Khalilzadeh [a,b,*], Mohammad Rashidi [c], Alireza Soleimanian [d], Habib Tajalli [e], Gulsah Saydan Kanberoglu [f], Behzad Baradaran [g], Mohammad-Reza Rashidi [c,h]

[a] Stem Cell Research Center (SCRC), Tabriz University of Medical Sciences, Tabriz, Iran
[b] Biosensors and Bioelectronics Research Center, Ardabil University of Medical Sciences, Ardabil, Iran
[c] Research Center for Pharmaceutical Nanotechnology (RCPN), Tabriz University of Medical Sciences, Tabriz, Iran
[d] Department of Biology, Faculty of Natural Sciences, University of Tabriz, Tabriz, Iran
[e] Biophotonic Research Center, Islamic Azad University, Tabriz Branch, Tabtiz, Iran
[f] Department of Chemistry, Faculty of Sciences, Van Yuzuncu Yil University, 65080, Van, Turkey
[g] Immunology Research Center, Tabriz University of Medical Sciences, Tabriz, Iran
[h] Faculty of Pharmacy, Tabriz University of Medical Sciences, Tabriz, Iran

ARTICLE INFO

Article history:
Received 27 February 2019
Received in revised form 7 May 2019
Accepted 8 May 2019
Available online 10 May 2019

Keywords:
Alzheimer
Biosensing
miR-146a
Biomedical analysis
Neurodegenerative
RNA

ABSTRACT

A MicroRNA (miR) based electrochemical method for quantification of miR-146a, a known biomarker for neurodegenerative disease, was developed. In this bioassay, the capture microRNA (C-miR) was self-assembled on the gold surface and used for quantification of target microRNA (T-miR) of miR-146a. For this purpose, an optimized concentration of C-miR was immobilized on the surface of gold electrode and used for capture of target analyte (T-miR). All of preparation steps were characterized by electrochemical techniques (cyclic voltammetry (CV) and electrochemical impedance spectroscopy (EIS)) and atomic force microscopy (AFM). At the optimized conditions, the linear dynamic range, limit of quantification and relative standard deviation of the proposed bioassay were obtained as 10 pM to 1 μM, 10 pM and 1.59%, respectively. The unprocessed human serum sample was used as a real sample and the results fully confirm that the designed microRNA based biosensor is capable for detection of miR-146a as neurodegenerative disease biomarker. The developed method offers a more precise and high sensitive tool to be used in clinical applications for early detection of neurodegenerative disease like Alzheimer's and Parkinson.

1. Introduction

Neurodegenerative diseases are types of brain and memory disorders in which the sufferers lose their brain functions during dementia (synaptic failure and neuron death). It is important to declare that, these diseases have special feature and that is silent progression of them [1]. Based on the statistical reports of WHO, today, approximately 45 million people suffering of dementia related diseases and the costs of diagnosis, treatment and monitoring of therapeutic efficacy of these disorders are growing terribly. Almost in the world, any year 10 million new cases of these disorders record and in other word, any new cases in about 4 s. One of the most challenging and age depended dementia disorders is Alzheimer's disease (AD), in which, two proteins (amyloid beta and tau) were involved [2,3]. Tau is a microtubule-associated protein and which was existing in its phosphorylated form in normal neuronal cell skeleton. Literature points the secretion of exosomal microRNAs into circulation during the pathological changes in brain such as Alzheimer's disease [4,5]. The aggregation process of dementia related proteins is highly correlated to their solvent specifics (temperature, pH and ionic strength) and also folding mechanisms [6,7]. Some co-solvents and osmolytes were applied for modifying the solvent conditions [8,9]. In addition, the secondary structure of proteins (α-helix and β-sheets) is highly involved in the aggregation process of AD mediated proteins [10]. Consequently, the unusual association of irregularly folded proteins directed to some toxic products and finally led to AD [11]. During last decades, the detection and diagnosis of neurodegenerative diseases was in a deadlock due to lack of ultrasensitive and high

* Corresponding author at: Stem Cell Research Center (SCRC), Tabriz University of Medical Sciences, 51666-14756 Tabriz, Iran.
E-mail address: khalilzadehb@tbzmed.ac.ir (B. Khalilzadeh).

https://doi.org/10.1016/j.ijbiomac.2019.05.061
0141-8130/

selective methods. While, nowadays, by using of recent progresses in nanotechnology most methods were used for early detection and diagnosis of neurodegenerative diseases, especially for Alzheimer's disease (mainly for Tau protein (TP)) [12]. The TP has critical role in the stabilization process of microtubules in normal neuronal cells systems. Abnormal hyperphosphorylation procedures of TP resulted in the TP dissociate from microtubules and consequently microtubules were disestablished. This disestablishment leads to formation of insoluble neurofibrillary tangles and finally, hyperphosphorylated TP were aggregated and neurodegenerative diseases occurred [13]. On the other hand, micro RNAs (miRs) as noncoding coding RNA have huge impact in molecular biology to inhibition of gene expression [14]. Interestingly, in the neuronal cells of Alzheimer diseases sufferers, the expression of miR-146a is upregulated and its pathway target is rho-associated, coiled-coil containing protein kinase 1 (ROCK1). Any reduction in the activity of ROCK1, resulted in, upregulation of miR-146a and consequently, the hyperphosphorylation process of TP will occurred in the other word, there is an opposite expression relation between the ROCK1 and miR-146a. Any reduction in the expression of miR-146a caused to falling in the hyperphosphorylation of TP and as a result, the Alzheimer's disease will knockdowned [15]. Different analytical methods and techniques were used for evaluation of expression, detection and quantification of miR-146a, like Real-time quantitative polymerase chain reaction (RT-qPCR) [16] and electrochemical [17]. In addition, the RT-qPCR methods [16] were mostly used for analyzing the expression of miRs and not for quantification. In some methods [17], the duplex-specific nuclease (DSN) enzyme was used for enzymatic reaction during analysis. As we know, the DNA-RNA complexes and DNA-DNA double strained were cleaved and separated from single strained DNAs and RNSs. An enzymatic reaction during electrode preparation may cause some contamination during analysis. Based on the discussed methods, our designed bioassay is free from any enzymatic reactions and quantitative results obtained for detection of miR-146a in comparison with RT-qPCR methods.

Self-assembled monolayers (SAMs) are flexible and sponges organic layers, which is highly oriented, regularly, and uniformly dispersed on some surfaces using covalent bonds [18]. In addition SAMs were categorized as nano layers, mostly were used for designing of electrochemical (on Au electrode [19] or on Au nanoparticles [20]) and electrochemiluminescence [21] based biosensors.

Electrochemical methods for their ultra-high sensitivity were used for designing of most types of sensors for quantification anti-inflammatory drug [22], anti-rheumatic drug [23] nano sensors for vitamin detection [24] and specially for biomaterials and amino acids [25]. Also electrochemical techniques because of their simplicity, low application cost and high response time, have been noticed by biological and medical researchers [26].

In Alzheimer's conditions, the miR-146a regulates the inflammation process via immune system complements [27]. MicroRNAs (miRs) based electrochemical biosensors are a special type of biosensors, in which, the designer used SAMs method for attachment of capture miRs on the electrode surfaces.

According to the mentioned top features about miR-146a and its essential role in the dementia related diseases pathways, ultrasensitive quantification of miR-146a is highly needed in clinical laboratories. In this work, miR based biosensing platform for detection of miR-146a was proposed. To the best of our knowledge, this work is the first miR based biosensor platform for indirect detection of TP hyperphosphorylation in dementia related disease, the specific C-miR and T-miR for sensitive indirect detection of hyperphosphorylation effect of TP was designed and synthesized. Bioconjugation between the capture and target miR caused to ultrasensitive detection of miR-146a as neurodegenerative disease biomarker. The SAMs method was used for attachment of C-miR on the gold surface and furthermore nanoconjugation between the C-miR and T-miR caused making an ultrasensitive biosensor platform for indirect detection of hyperphosphorylation in TP. Phosphate buffered saline (PBS) was prepared by dissolving specific amount of KCl, NaCl, Na_2HPO_4 and KH_2PO_4 salts.

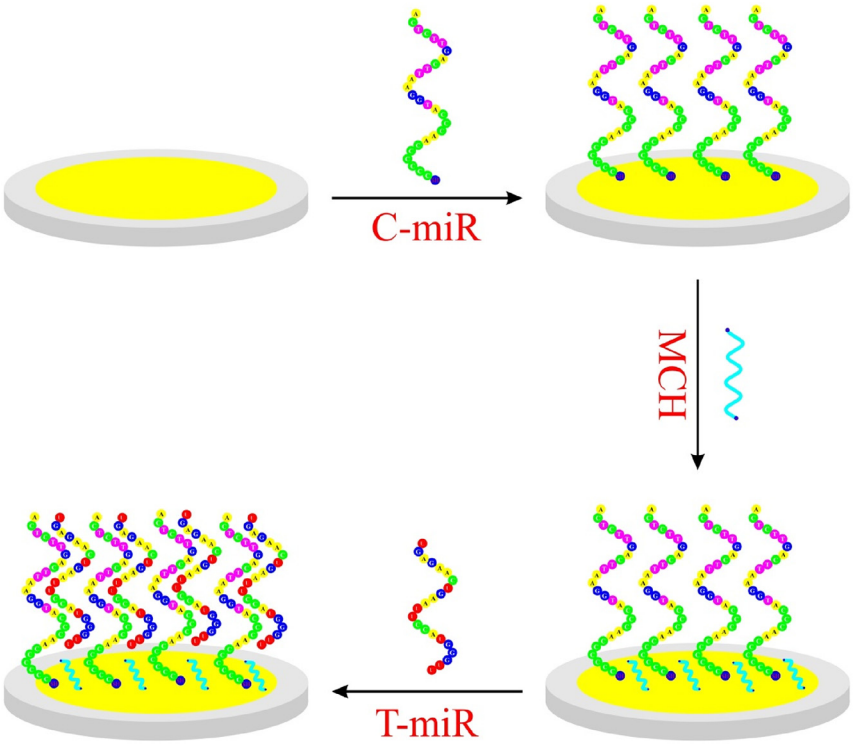

Scheme 1. The electrode preparation steps.

2. Experimental

2.1. Material and methods

All of the materials were analytical grade and used without any purification. The C-miR and T-miR were purchased from in lyophilized form. 6-mercapto-1-hexanol (MCH), potassium ferrocyanide, potassium chloride, sulfuric acid, nitric acid and sodium hydroxide were obtained from Sigma Company, USA. All the solutions were prepared in double distilled water. The C-miR sequence was 5′-HS-CCCCCCAACCCATGGAATTCAGTTCTCA-3′ and the T-miR sequence was 5′-UUGGGUACCUUAAGUCAAGAGU-3′. The T-miR-MCH-C-miR gold electrode was used as working electrode. The platinum wire (Pt) and Ag/AgCl electrodes were used as counter and reference electrode respectively. All the potentials were compared to the reference electrode. All of the electrodes were used in the electrochemical cell and its current and potentials were controlled by NOVA 2.1 software. All of the electrochemical techniques like; cyclic voltammetry (CV), square wave voltammetry (SWV), leaner reductive sweep voltammetry (LSV (RED)) and electrochemical impedance spectroscopy (EIS) were perform on the autolab electrochemical work station system (PGSTAT302N, the Netherlands). All of the AFM images were taken by Nanosurf Mobile S, Switzerland. The schematic diagram of the electrode preparation steps was presented in Scheme 1.

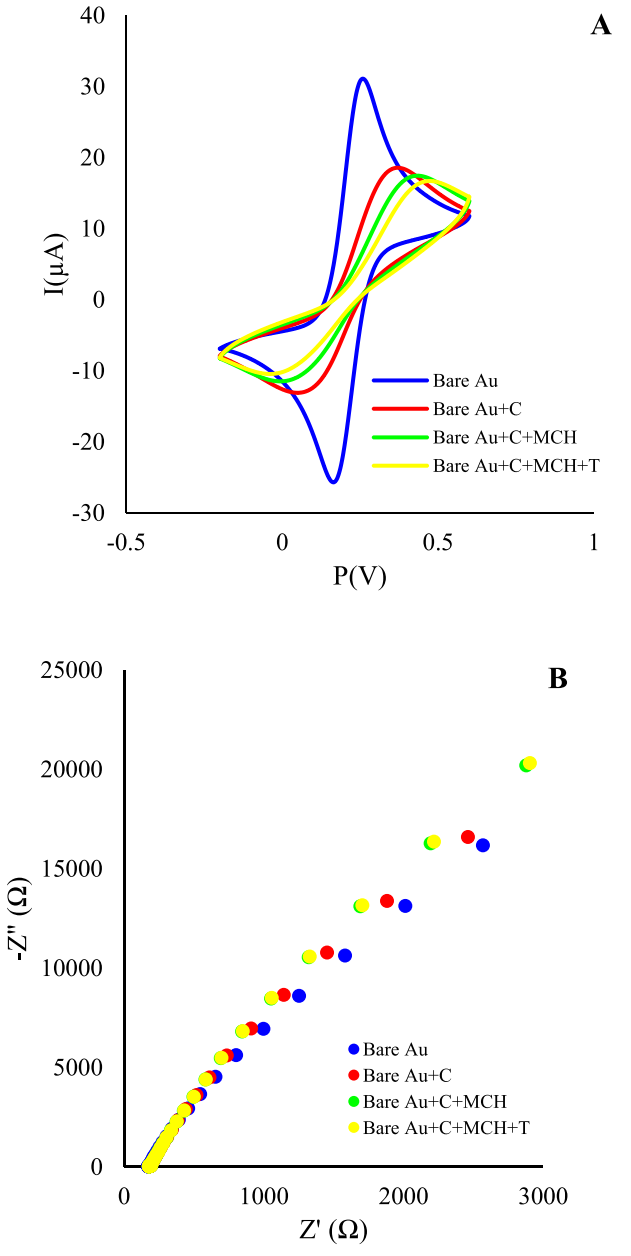

Fig. 1. A) CVs and B) EIS of RNA biosensor assembling for Au electrode before and after modification by C-miR, C-miR + MCH, and C-miR + MCH + T-miR.

3. Results and discussion

3.1. RNA biosensor assembling

The Au electrode was physically and electrochemically cleaned. Briefly, the Au electrode was washed with nitric acid 2% (v/v), double distilled water and acetone, respectively. Then, the Au electrode was polished on the polishing pad and colloidal slurry of alumina with double distillated water to producing mirror like surface of Au electrode. Afterword, the physically pre-cleaned Au electrode, was prepared to electrochemically cleaning steps. In brief, the physically pre-cleaned Au electrode was put in the electrochemical cell containing sulfuric acid 0.5 M and cyclic voltammetry technique was used for cycling of potential between −0.30 to 1.50 V, scan rate 100 mV/s til reaching a repetitive voltammograms. After cleaning, capture probe (CP, 20 μL, 75 μM) was drop on the Au electrode and incubated at 37 °C for 4 h, in 100% humidity condition. Interestingly, TCEP compound was used for preventing of disulfide bond formation at the end of the designed CP. Thereafter, for getting the repeatable data, the unreacted parts of the electrode blocked with 6-mercapto-1-hexanol (MCH, 120 μL, 1 mM) at room temperature (RT) for 1 h. Importantly, the modified electrode with CP was washed with PBS (pH = 7.4) after and before blocking with MCH (for better removing of physically adsorbed CPs on the Au electrode). Then, the modified electrode was incubated with portion of target probe (TP, 15 μL, 75 μM) at 37 °C for 4 h. All of the electrode preparation steps were characterized by CV and EIS techniques. The corresponding CV voltammograms and EIS curves were illustrated in Fig. 1A and B, respectively. The electrode preparation steps were completely confirmed by the results of atomic force microscopy (AFM).

3.2. Atomic force microscopy (AFM) analysis

The surface topography and roughness of the Au electrode and also all electrode preparation steps were characterized and confirmed by AFM. Based on the AFM images were presented in Fig. 2, the Au electrode presents some roughness about, 25 nm. After addition of C-miR on the Au electrode, the topology of the Au electrode was changed and about 25 nm enhanced and reached to 48.4 nm. In this situation, some of C-miR may have specific folding and some bending in their structure. After casting of MCH on the C-miR modified electrode, the MCH molecule because of its small structure in length, could easily self-assembled on the Au electrode and consequently, the folding and bending helical structure a little disrupted and resulted in, the surface characters were altered and the roughness obtained as 69.6 nm. Finally, after incubation of T-miR on the modified electrode, the roughness was increased again and reached to 90.2 nm. All of the recorded data are in consistence with CV and EIS data for electrochemical preparation steps and completely confirm that the electrode was successfully constructed.

3.3. Optimization of experimental variables

3.3.1. Capture probe concentration

One of the most important variables in the optimization of the designed miR based biosensor is capture probe concentration which was

deposited on the Au electrode. CV technique was used for optimization of capture probe optimization. According to the Fig. 3A, the CVs of different concentration of the C-miR were compared by Au electrode. Based on these results Fig. 3B, by increasing of the concentration of C-miR (2 μL to 10 μL), both oxidation and redox peaks of Fe^{+3} and Fe^{+2} were decreased correspond to increasing of the C-miR concentrations. So, one can conclude that, 10 μL C-miR completely covering the Au electrode. As illustrated in the Fig. 3 the concentration of 10 μL of C-miR was chosen as optimum concentration of C-miR for next optimization steps.

3.3.2. Capture probe incubation temperature

Another essential parameter in the designing of the miR based electrochemical biosensors is optimization of incubation temperature. The leaner reductive sweep voltammetry (LSV(RED)) technique was used for optimization of C-miR incubation temperature on the Au electrode. As presented in Fig. 4A, three temperature (−4 °C, room temperature (RT) and 37 °C) were used for optimization of C-miR incubation temperature using humidified atmosphere. Based on the presented CVs, by increasing of the incubation temperature, the peak currents of the self-assembled C-miR on the Au electrode were decreased and it can conclude that, the self-assembling process of C-miR via Au-sulphur dative bond on the Au electrode were slightly become stronger by increasing the incubation temperature. The results of incubation temperature were illustrated in bar chart (Fig. 4B). The results of LSV(RED) was completely confirmed by EIS technique. According to the Fig. 4C, by increasing the incubation temperature, the attachment of the C-miR was enhanced, on the other hand, the diameter of the semicircle part of the EIS spectra, a little increased and confirmed the CV results.

3.3.3. Capture probe incubation time

The third parameter which was optimized during designing of the proposed biosensor was incubation time of C-miR on the Au

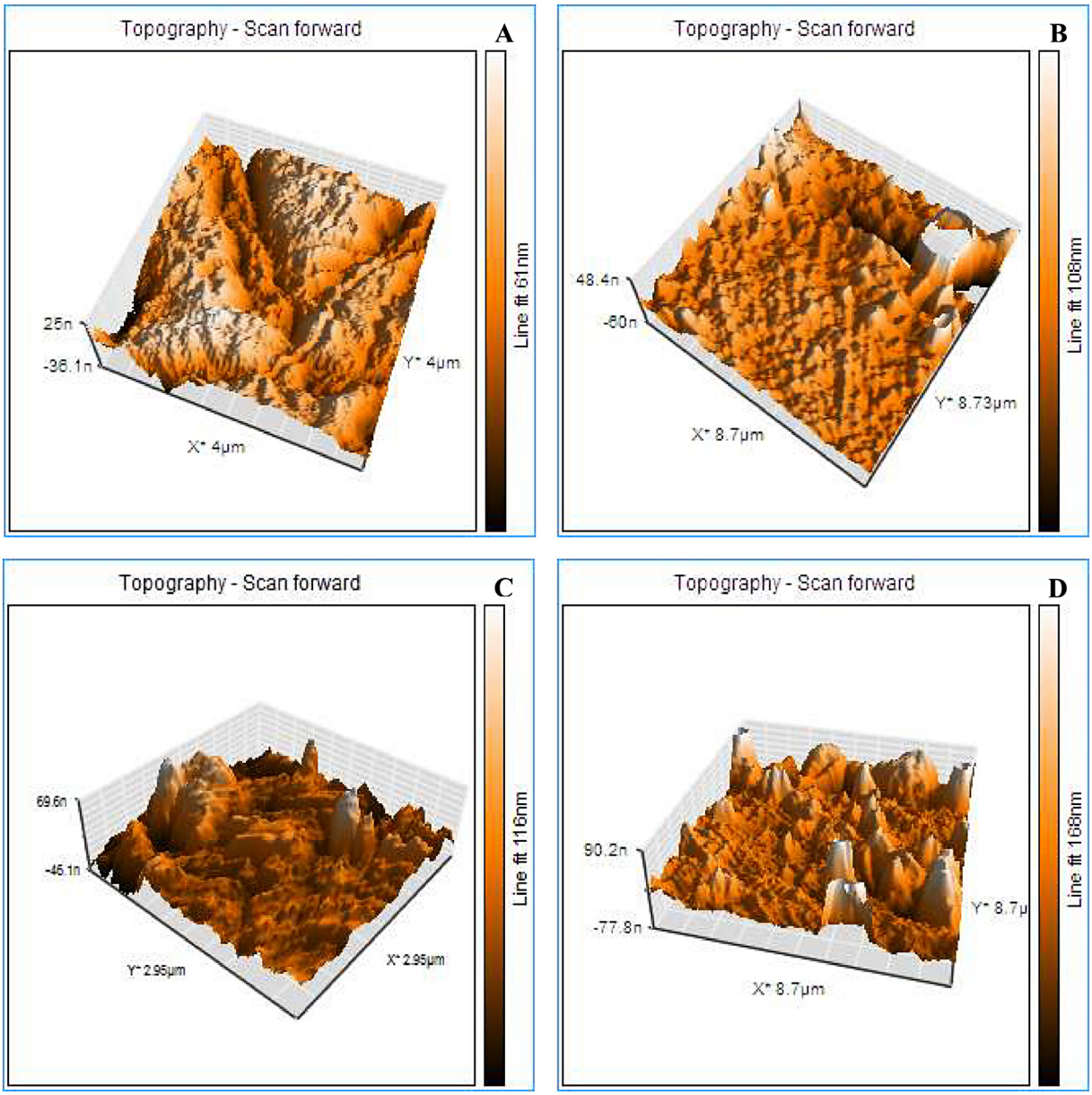

Fig. 2. A-D) The AFM topography images of Au electrode before (A) and after modification by C-miR (B), C-miR + MCH(C), and C-miR + MCH + T-miR(D), respectively.

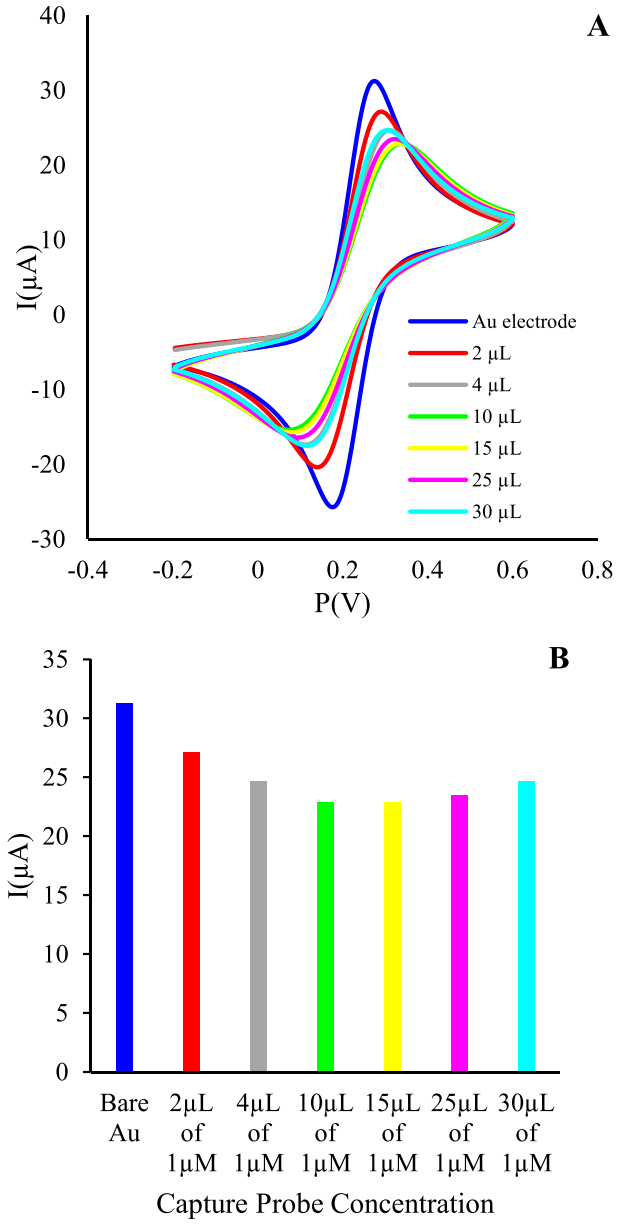

Fig. 3. A) CVs of capture probe in different concentrations (0, +2 μL, +4 μL, +10 μL, +15 μL, +25 μL and + 30 μL of 1 μM capture probe. B) Histogram of the capture probe concentrations.

electrode. The CV and EIS techniques were used for optimization of C-miR incubation time on the Au electrode. According to the results presented in the Fig. 5A, B and C, the incubation time were optimized during 1 to 24 h. By increasing the incubation time, both oxidation and redox peaks of Fe^{2+} to Fe^{3+} and Fe^{3+} to Fe^{2+} were decreased. Based on the EIS spectra were illustrated in the Fig. 5B, by increasing the incubation time to 4 h, the charge transfer resistance (R_{ct}) was increased and after that the results were reached a plateau. Consequently, 4 h was chose as optimum incubation time of C-miR on the Au electrode. It is important to point out that, the results of CV and EIS were completely confirming each other.

3.3.4. Target probe incubation temperature

The CV technique was used for optimization of target prone incubation temperature. Three temperatures (4 °C, RT and 37 °C)

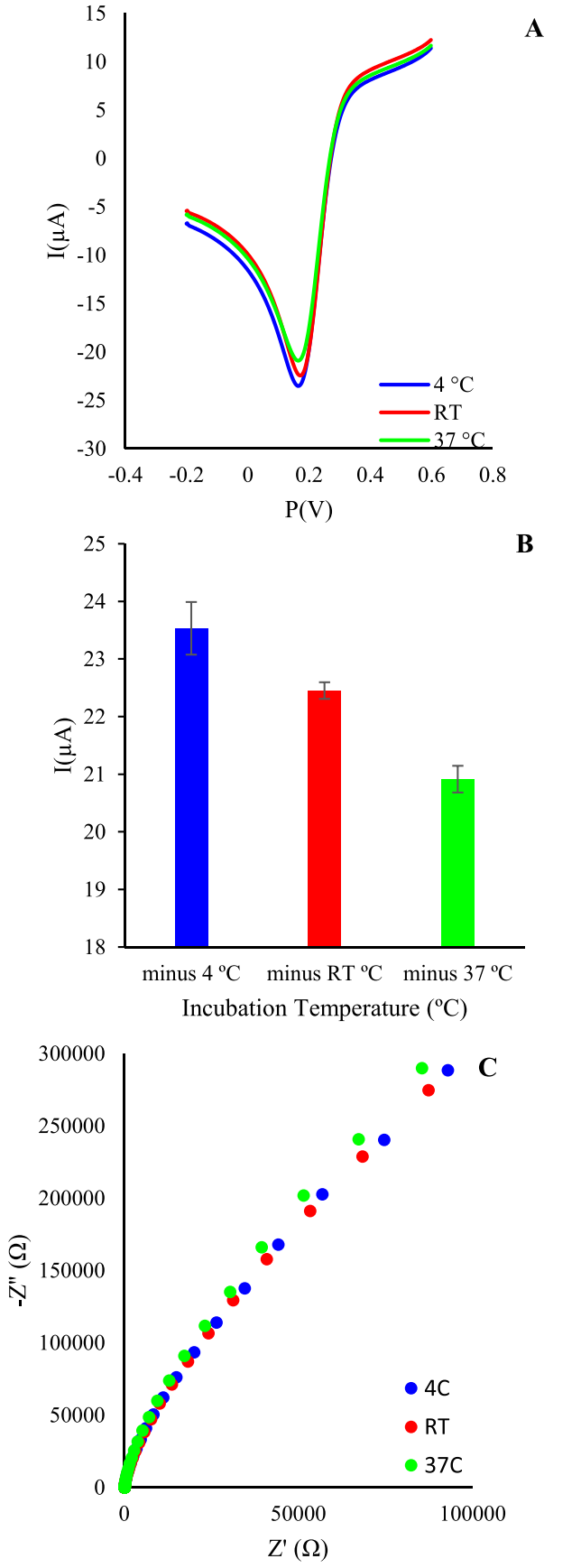

Fig. 4. A) LSV(RED); B) histograms; and C) EIS of capture probe incubation temperature (4 °C, room temperature (24 °C) and 37 °C).

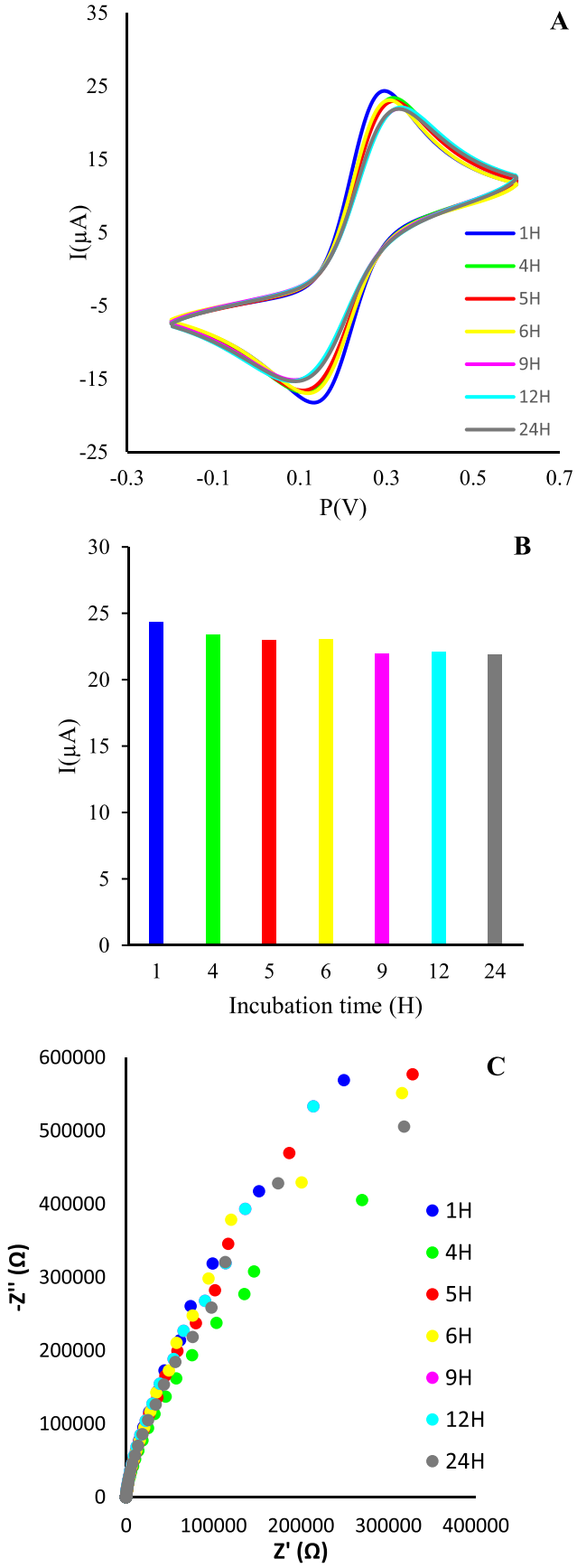

Fig. 5. A) CVs; B) histogram; and C) EIS of capture probe incubation time (1, 4, 5, 6, 9, 12 and 24 h).

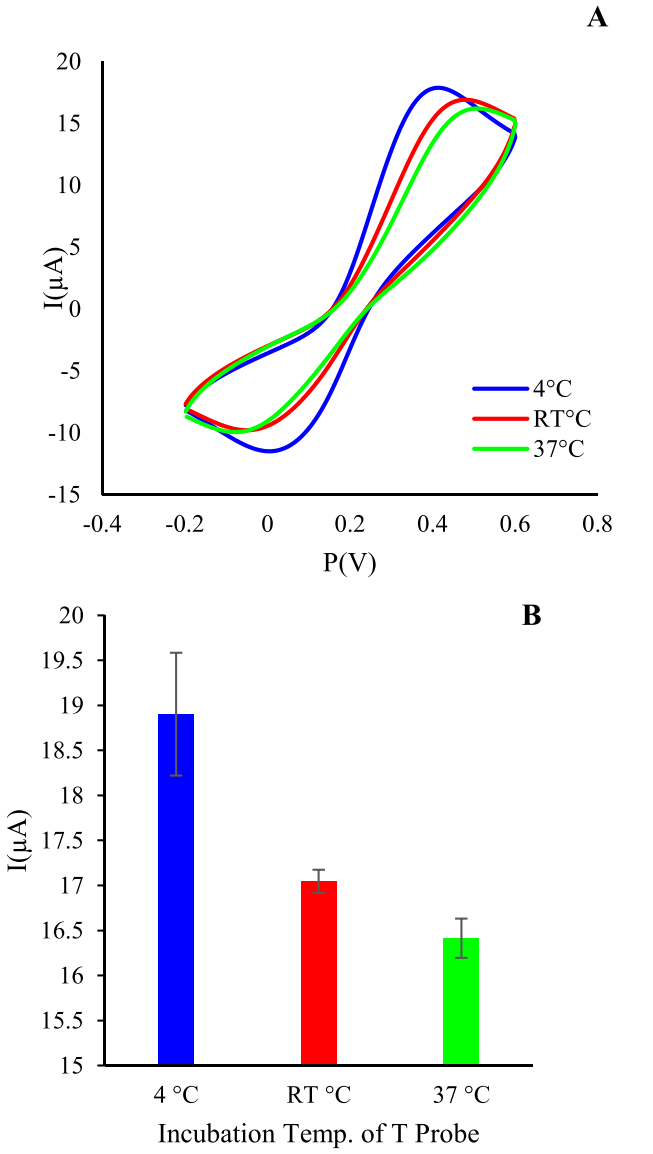

Fig. 6. A) CVs; and B) histogram of target probe incubation temperature (4 °C, room temperature and 37 °C).

were selected for this optimization parameter. The cyclic voltammograms were presented in Fig. 6A and corresponding bar charts were illustrated in Fig. 6B as can be seen, the oxidation and reduction peaks currents of Fe^{2+} and Fe^{3+} were decreased by increasing of the incubation temperature. Based on the presented voltammograms and histogram, the 37 °C was selected as the best incubation temperature for target probe. Importantly, the incubation process was suitable in the humidified systems and caped for preservation of evaporation.

3.3.5. Target probe incubation time

Finally, target probe incubation time was optimized using CV technique, which was shown in Fig. 7A. According to the existing voltammograms and resultant histogram (Fig. 7B), by increasing the incubation time of TP, the reduction peak currents were decreased. Finally, the 4 h incubation time was nominated as the optimal incubation time for TP.

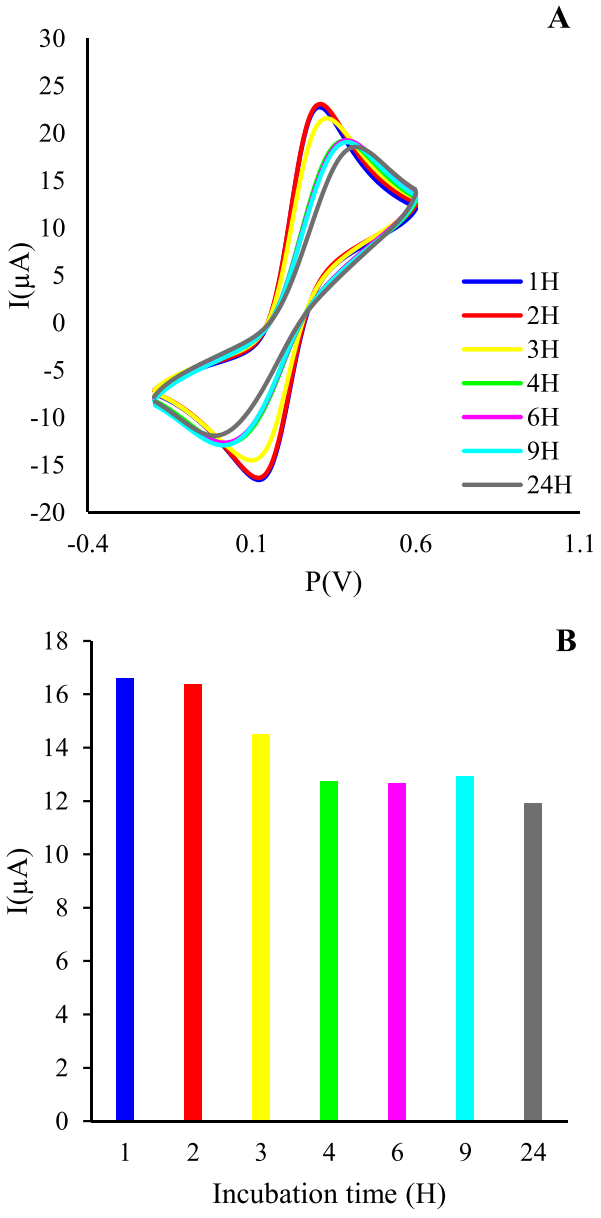

Fig. 7. A) CVs, and B) histogram of target probe incubation time (1, 2, 3, 4, 6, 9 and 24 h).

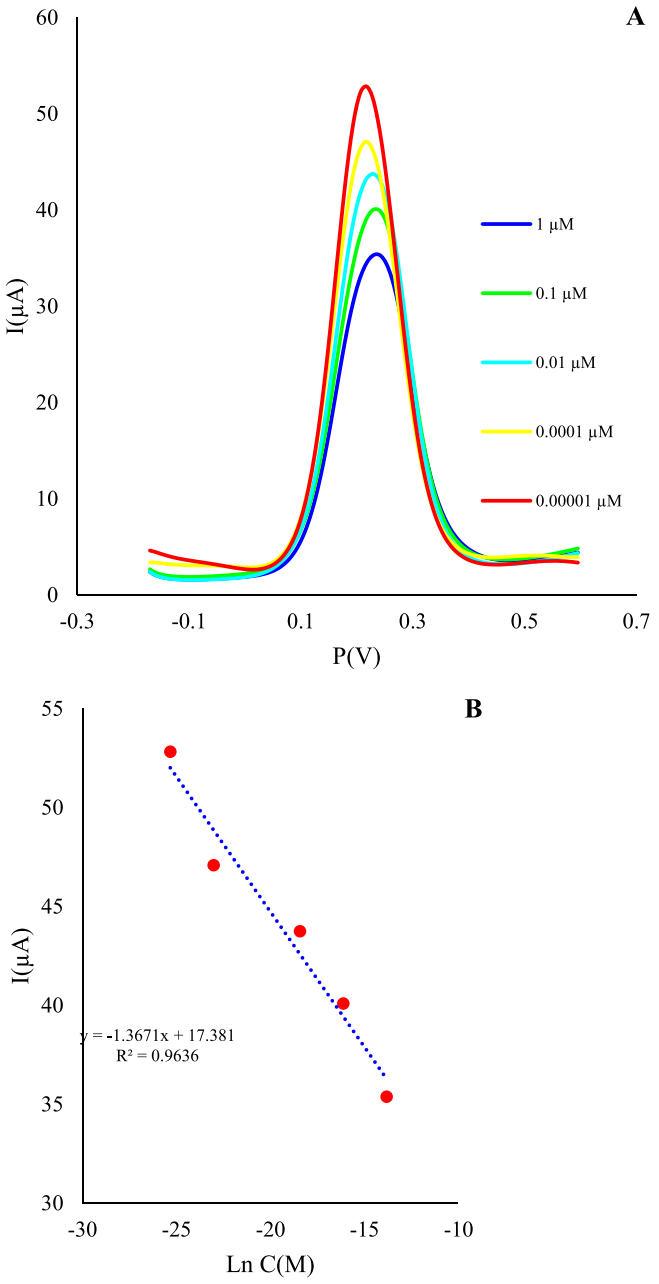

Fig. 8. A) SWVs of Au electrode modified by C-miR + MCH + T-miR in different concentrations of miR-146a (1, 0.1, 0.01, 0.0001 and 0.00001 μM). B) Calibration curve of the prepared biosensor.

4. Analytical approach

4.1. Calibration curve

The SWV technique was used for drawing of electrochemical response to concentration of the developed miR based biosensor was showed in Fig. 8A and B. Based on the presented SWVs, by increasing the concentration of the T-miR, the SWV peak currents, were correspondingly decreased. According to the calibration curve (Fig. 8B), the equation of I(μA) = 1.3671 Ln(C(T-miR)) + 17.381 and its R^2 was obtained as 0.9636. The linear dynamic range (LDR) and limit of detection were obtained as 10 pM to 1 μM and 10 pM, respectively.

4.2. Precision

The precision of the designed miR based biosensor was checked using relative standard deviation (RSD) of the obtained data with SWV. The electrode was prepared using 0.1 nM of T-miR and the final modified electrode (T-miR-MCH-C-miR-Au electrode) was used for this examination by SWV for 50 times. The SWVs was illustrated in Fig. 9, based on the data was extracted form SWVs, the RSD obtained as 1.59% and this result completely confirm that the designed miR based biosensor is very precise and repeatable.

4.3. Real sample analysis

The best and important feature of the biosensors is their application in real samples. For this aim, the unprocessed human serum

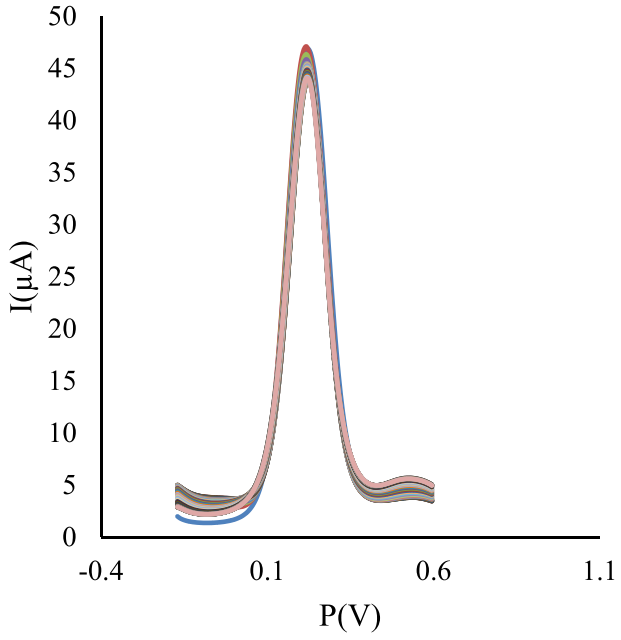

Fig. 9. SWVs of 50 repetitive record of 0.1 nM of target probe.

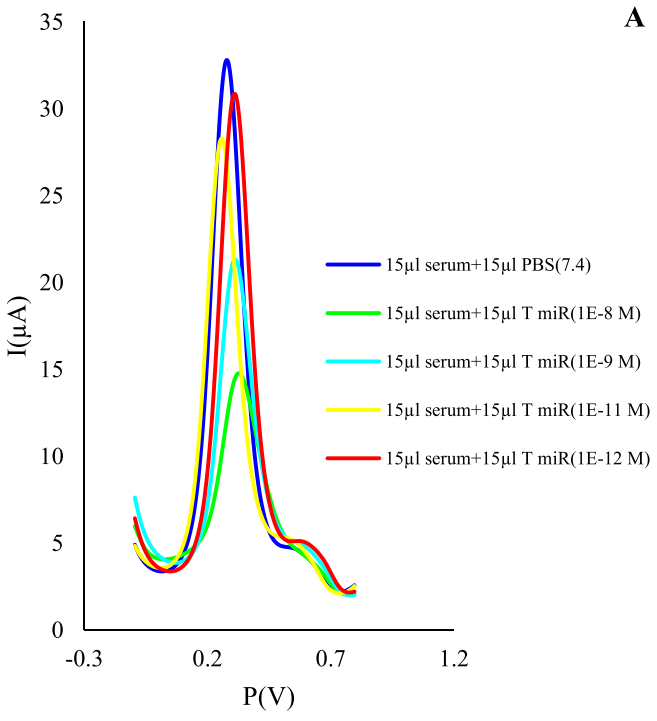

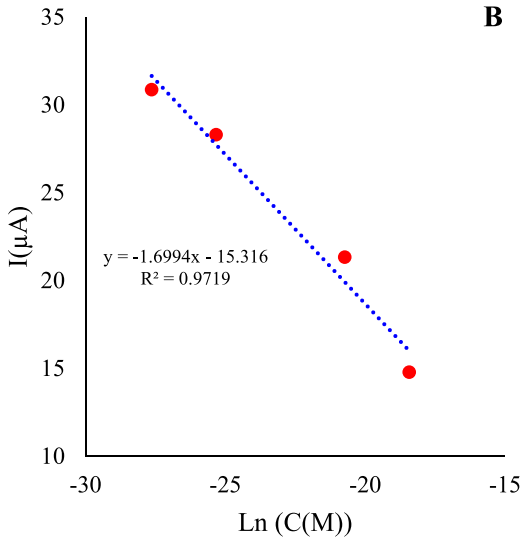

Fig. 10. A) SWVs of Au electrode modified by C-miR + MCH + T-miR in different concentrations of miR-146a (0.01, 0.001, 0.00001 and 0.000001 μM) in the presence of 15 μL human plasma sample. B) Calibration curve of the prepared biosensor.

sample was used for qualification of the designed biosensor. The specific concentrations of T-miR were mixed with equal volume of unprocessed human serum samples (15 μL) without any intervention and dilution. The pre-cleaned Au electrode was incubated with the C-miR and MCH according to the electrode preparation steps and in the incubation step with T-miR, the T-miR and human serum samples were mixed each other and the mixer was caste on the modified electrode (spike method). Then, the SWV of the developed biosensor was recorded in the same conditions of the calibration curve. As presented in Fig. 10A and B, by increasing the concentration of spiked T-miR in the serum sample, the peak current of SWVs were decreased. Based on the recorded data, the designed miR based biosensor, capable to use as robust and simple biosensor for early detection of neurodegenerative diseases like Alzheimer's and Parkinson's in clinical tests.

5. Conclusion

In summary, in this biodesigning, a special micro RNA was designed for the detection of miR-146a as specific marker of TP. The developed reliable biosensor is highly capable to detection of TP as Alzheimer's diseases at the low concentration (10 pM). This early detection of neurodegenerative diseases biomarker will cause to more decrease in the dementia related casts. One of the top features of this biosensing is its application in unprocessed serum samples. We hope that, in the future studies, we could detect this biomarker in the peripheral blood samples. This nanoconjugation process can be easily performed on the chips and it has ability to make commercial electrical kit and use in clinical laboratories. Finally, this biosensor is very sensitive and selective. The obtained data of the present bioassay system is very precise and stable.

Acknowledgment

The authors are greatly thanked to Stem Cell Research Center (SCRC), Tabriz University of Medical Sciences for the financial support of this project.

References

[1] J.J. Palop, J. Chin, L. Mucke, A network dysfunction perspective on neurodegenerative diseases, Nature 443 (2006) 768.
[2] B. Duthey, Alzheimer's Disease (AD), World Health Organization, 2013 Retrievedfrom.
[3] R. Melki, Role of different alpha-synuclein strains in synucleinopathies, similarities with other neurodegenerative diseases, J. Park. Dis. 5 (2) (2015) 217–227.
[4] M. Majidinia, A. Mihanfar, R. Rahbarghazi, A. Nourazarian, B. Bagca, Ç.B. Avci, The roles of non-coding RNAs in Parkinson's disease, Mol. Biol. Rep. 43 (11) (2016) 1193–1204.
[5] J. Rezaie, S. Ajezi, Ç.B. Avci, M. Karimipour, M.H. Geranmayeh, A. Nourazarian, E. Sokullu, A. Rezabakhsh, R. Rahbarghazi, Exosomes and their application in biomedical field: difficulties and advantages, Mol. Neurobiol. 55 (4) (2018) 3372–3393.
[6] M.V. Khan, G. Rabbani, E. Ahmad, R.H. Khan, Fluoroalcohols-induced modulation and amyloid formation in conalbumin, Int. J. Biol. Macromol. 70 (2014) 606–614.
[7] A. Varshney, G. Rabbani, G. Badr, R.H. Khan, Cosolvents induced unfolding and aggregation of keyhole limpet hemocyanin, Cell Biochem. Biophys. 69 (1) (2014) 103–113.

[8] M.V. Khan, G. Rabbani, M. Ishtikhar, S. Khan, G. Saini, R.H. Khan, Non-fluorinated cosolvents: a potent amorphous aggregate inducer of metalloproteinase-conalbumin (ovotransferrin), Int. J. Biol. Macromol. 78 (2015) 417–428.
[9] G. Rabbani, I. Choi, Roles of osmolytes in protein folding and aggregation in cells and their biotechnological applications, Int. J. Biol. Macromol. 109 (2018) 483–491.
[10] P. Sen, B. Ahmad, G. Rabbani, R.H. Khan, 2,2,2-Trifluroethanol induces simultaneous increase in α-helicity and aggregation in alkaline unfolded state of bovine serum albumin, Int. J. Biol. Macromol. 46 (2) (2010) 250–254.
[11] T.I. Chandel, M. Zaman, M.V. Khan, M. Ali, G. Rabbani, M. Ishtikhar, R.H. Khan, A mechanistic insight into protein-ligand interaction, folding, misfolding, aggregation and inhibition of protein aggregates: an overview, Int. J. Biol. Macromol. 106 (2018) 1115–1129.
[12] H.-G. Jahnke, D. Krinke, D. Seidel, K. Lilienthal, S. Schmidt, R. Azendorf, M. Fischer, T. Mack, F. Striggow, H. Althaus, A. Schober, A.A. Robitzki, A novel 384-multiwell microelectrode array for the impedimetric monitoring of Tau protein induced neurodegenerative processes, Biosens. Bioelectron. 88 (Supplement C) (2017) 78–84.
[13] J.O. Esteves-Villanueva, H. Trzeciakiewicz, S. Martic, A protein-based electrochemical biosensor for detection of tau protein, a neurodegenerative disease biomarker, Analyst 139 (11) (2014) 2823–2831.
[14] M. Mahdipour, H.T. van Tol, T.A. Stout, B.A. Roelen, Validating reference microRNAs for normalizing qRT-PCR data in bovine oocytes and preimplantation embryos, BMC Dev. Biol. 15 (1) (2015) 25.
[15] G. Wang, Y. Huang, L.-L. Wang, Y.-F. Zhang, J. Xu, Y. Zhou, G.F. Lourenco, B. Zhang, Y. Wang, R.-J. Ren, G.M. Halliday, S.-D. Chen, MicroRNA-146a suppresses ROCK1 allowing hyperphosphorylation of tau in Alzheimer's disease, Sci. Rep. 6 (2016) 26697.
[16] K. Jazdzewski, S. Liyanarachchi, M. Swierniak, J. Pachucki, M.D. Ringel, B. Jarzab, A. de la Chapelle, Polymorphic mature microRNAs from passenger strand of pre-miR-146a contribute to thyroid cancer, Proc. Natl. Acad. Sci. 106 (5) (2009) 1502–1505.
[17] Y. Lei, Y. Fan, D. Yuanlin, Y. Haibin, Y. Lin, D. Qi, S. Yujie, W. Xiaoxue, X. Yang, Z. Guo-Jun, Bioinspired trans-scale functional interface for enhanced enzymatic dynamics and ultrasensitive detection of microRNA, Adv. Funct. Mater. 28 (17) (2018), 1706981.
[18] A. Ulman, Formation and structure of self-assembled monolayers, Chem. Rev. 96 (4) (1996) 1533–1554.
[19] B. Khalilzadeh, N. Shadjou, M. Eskandani, H.N. Charoudeh, Y. Omidi, M.-R. Rashidi, A reliable self-assembled peptide based electrochemical biosensor for detection of caspase 3 activity and apoptosis, RSC Adv. 5 (72) (2015) 58316–58326.
[20] B. Khalilzadeh, H.N. Charoudeh, N. Shadjou, R. Mohammad-Rezaei, Y. Omidi, K. Velaei, Z. Aliyari, M.-R. Rashidi, Ultrasensitive caspase-3 activity detection using an electrochemical biosensor engineered by gold nanoparticle functionalized MCM-41: its application during stem cell differentiation, Sensors Actuators B Chem. 231 (2016) 561–575.
[21] B. Khalilzadeh, N. Shadjou, H. Afsharan, M. Eskandani, H. Nozad Charoudeh, M.-R. Rashidi, Reduced graphene oxide decorated with gold nanoparticle as signal amplification element on ultra-sensitive electrochemiluminescence determination of caspase-3 activity and apoptosis using peptide based biosensor, Bioimpacts 6 (3) (2016) 135–147.
[22] N. Aliakbarinodehi, F. Stradolini, S.A. Nakhjavani, I. Tzouvadaki, I. Taurino, G.D. Micheli, S. Carrara, Performance of carbon nano-scale allotropes in detecting midazolam and paracetamol in undiluted human serum, IEEE Sensors J. 18 (12) (2018) 5073–5081.
[23] B. Khalilzadeh, M. Hasanzadeh, S. Sanati, L. Saghatforoush, N. Shadjou, J.E.N. Dolatabadi, P. Sheikhzadeh, Preparation of a new electrochemical sensor based on cadmium oxide nanoparticles and application for determination of penicillamine, Int. J. Electrochem. Sci. 6 (2011) 4164–4175.
[24] G. Karim-Nezhad, M. Hasanzadeh, L. Saghatforoush, N. Shadjou, B. Khalilzadeh, S. Ershad, Electro-oxidation of ascorbic acid catalyzed on cobalt hydroxide-modified glassy carbon electrode, J. Serb. Chem. Soc. 74 (5) (2009) 581–593.
[25] B. Khalilzadeh, M. Hasanzadeh, B. Bakhoday, A. Babaei, M. Hajjizadeh, M. Zendehdel, Zeolite nanoparticles-modified carbon paste electrode as a biosensor for simultaneous determination of tryptophan and dopamine, J. Chin. Chem. Soc. 56 (2009) 789–796.
[26] S.A. Nakhjavani, B. Khalilzadeh, P.S. Pakchin, R. Saber, M.H. Ghahremani, Y. Omidi, A highly sensitive and reliable detection of CA15-3 in patient plasma with electrochemical biosensor labeled with magnetic beads, Biosens. Bioelectron. 122 (2018) 8–15.
[27] F. He, B. Liu, Q. Meng, Y. Sun, W. Wang, C. Wang, Modulation of miR-146a/complement factor H-mediated inflammatory responses in a rat model of temporal lobe epilepsy, Biosci. Rep. 36 (6) (2016).